



Outcrop-scale physical properties of Burns Formation at Meridiani Planum, Mars

Amanda L. Nahm¹ and Richard A. Schultz¹

Received 22 June 2007; revised 23 August 2007; accepted 5 September 2007; published 24 October 2007.

[1] A rock mass rating (RMR) analysis was performed on an outcrop of Burns Formation at Meridiani Planum, Mars. RMR values were calculated for the present dry conditions (RMR = 63) and past wet conditions (RMR = 52). For present-day dry conditions, the rock mass has an in situ modulus of deformation (E^*) of 21.1 GPa, cohesive strength (C_0^*) of 4.64 MPa, and tensile strength (T_0^*) of -0.24 MPa. These values were reduced by at most $\sim 50\%$ during previous water-saturated conditions. The critical grain crushing pressure (P^*) for dry conditions is 19.5 GPa, with an uncertainty of about an order of magnitude. Analysis of the rover observations indicates that the physical properties of Burns Formation are in the range of analogous terrestrial porous rock masses such as sandstone and shale. **Citation:** Nahm, A. L., and R. A. Schultz (2007), Outcrop-scale physical properties of Burns Formation at Meridiani Planum, Mars, *Geophys. Res. Lett.*, *34*, L20203, doi:10.1029/2007GL031005.

1. Introduction

[2] The objective of this paper is to determine physical properties of materials at the outcrop-scale on Mars observed by the Mars Exploration Rover *Opportunity*. RMR is commonly used by geological engineers to assess the rock strength and deformability (i.e., modulus) of a rock mass, which includes intact rock material, fractures, and pore fluid, for applications such as tunnels, slopes, foundations, and mines [Bieniawski, 1989]. The approach allows standardization of rock mass strength analysis so that one outcrop can be compared to another, regardless of age, location, or composition. Analysis of Martian outcrops using rock mass classification schemes is important to engineers and scientists developing future missions to Mars. Although this technique has been used extensively on Earth and on Martian rock masses using orbital data [Okubo and Schultz, 2004; Neuffer and Schultz, 2006], it has not been applied to an outcrop that has been characterized by in situ data on Mars until now. *Opportunity*, with its high-resolution images over a broad area, presents a unique chance to apply this technique to Martian materials.

2. Outcrop Description

[3] The outcrop studied was imaged on March 8, 2005 (sol 399; 1 sol = 1 Martian day) and is located within Vostok

crater near the rim at Meridiani Planum, Mars (Figure 1). All outcrops at the surface of Meridiani Planum are the upper unit of the Burns Formation [Squyres *et al.*, 2006]. The term “Burns Formation” refers to exposures of rock explored by *Opportunity* [Grotzinger *et al.*, 2005]. The Burns Formation at Meridiani Planum records a rich history of past aqueous surface and subsurface processes on Mars [Grotzinger *et al.*, 2005; Squyres and Knoll, 2005]. The thickness of the formation is estimated to be at least 10 m at Meridiani Planum [Grotzinger *et al.*, 2005], and 7 m are exposed in Endurance crater [Grotzinger *et al.*, 2005; Squyres and Knoll, 2005], with the total thickness of the unit in Terra Meridiani estimated to be as much as 600 m [Hynek *et al.*, 2002]. For detailed stratigraphy of the Burns Formation, see Grotzinger *et al.* [2005]. An upper bound for the age of the Burns Formation can be determined from analyses of orbital images that show the Meridiani Planum materials disconformably overlie Middle to Late Noachian cratered terrains [Hynek *et al.*, 2002]. This suggests that these plains materials could be as old as Late Noachian (~ 3.7 Ga) [Hynek *et al.*, 2002; Squyres *et al.*, 2004a].

[4] The Burns Formation is interpreted to be a sequence of sedimentary rocks formed in a wind-swept, arid surface environment with a variable water table [Squyres and Knoll, 2005]. Water rose to the surface at times and formed pools in which evaporation produced sulfate-rich sand grains that were transported by the wind to form sand dunes and sheets [Squyres and Knoll, 2005]. This sequence records a transition from dunes to dune marginal sand sheets to ephemeral pools of water at the surface [Squyres and Knoll, 2005]. Multiple episodes of ground water infiltration governed diagenesis, including the formation of the hematite concretions [Squyres and Knoll, 2005].

[5] As in other areas south of the Eagle crater landing site, the outcrop is covered with a veneer of basaltic eolian sand dunes and ripples [Grotzinger *et al.*, 2005; Squyres *et al.*, 2006]. This abundant unconsolidated regolith partially covers outcrops in the region and has partially filled in the joints, as well as Vostok crater itself.

[6] In the study area located ~ 1.6 km from the landing site, there are ~ 100 joints ranging in length from a few millimeters to ~ 1 m. Joints, defined as fractures with evidence of predominantly opening displacement (following Pollard and Aydin [1988]), may have formed by some combination of desiccation or weathering at the present day surface [McLennan *et al.*, 2005; Squyres *et al.*, 2006; Grotzinger *et al.*, 2006; Chan *et al.*, 2007], impact [McLennan *et al.*, 2005; Squyres *et al.*, 2006], diagenesis [Grotzinger *et al.*, 2005; McLennan *et al.*, 2005] or tectonism. The fracture networks on the rock surfaces commonly

¹Geomechanics-Rock Fracture Group, Department of Geological Sciences and Engineering, University of Nevada, Reno, Nevada, USA.

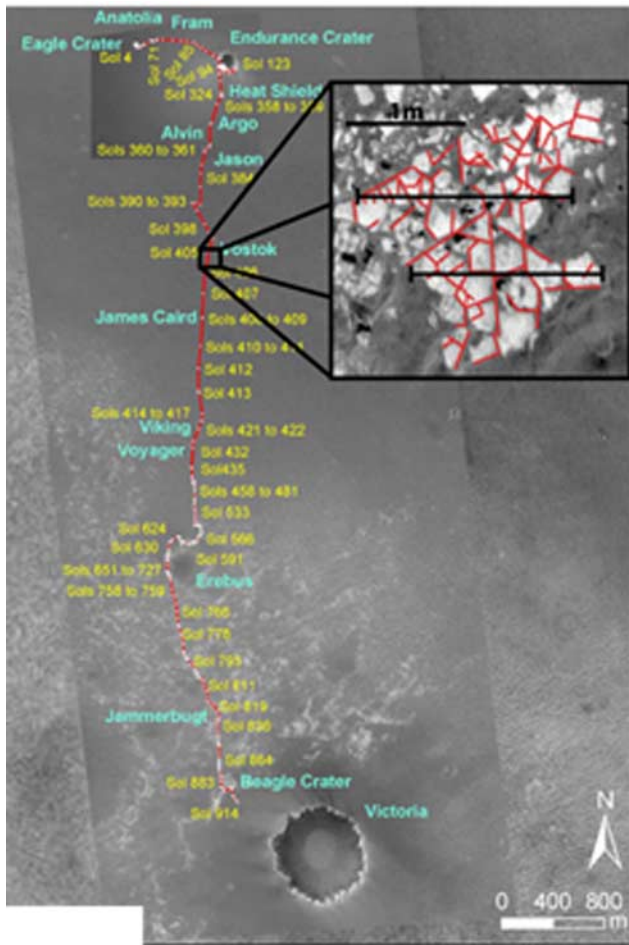


Figure 1. Map showing approximate location of the outcrop along *Opportunity's* traverse (red line). The outcrop is enlarged and shown in overhead view in the inset frame with joints mapped in red and the eRQD traverses for the RMR analysis shown as black lines. White scale bar is for the base image and the black scale bar applies to the inset outcrop map. Base image taken by the Mars Orbiter Camera (MOC) and courtesy of the Ohio State University Mapping and GIS Laboratory/MSSS and inset image taken by *Opportunity's* navigation camera (NAVCam) and courtesy of NASA/JPL (<http://marsrovers.jpl.nasa.gov/gallery/press/opportunity/20050315a.html>).

cut bedding [Squyres *et al.*, 2006] as at Burns Cliff in Endurance crater [Grotzinger *et al.*, 2005].

3. Assessment of Outcrop Properties

[7] There are six factors to be assessed when performing an RMR analysis. These are intact rock strength (unconfined compressive strength (UCS)), linear fracture density (or equivalent rock quality designation (eRQD)), average fracture spacing, fracture condition, groundwater conditions, and fracture orientation. Since the parameters are not equally weighted for RMR classification, importance ratings are given to different value ranges of the parameters, with higher values indicating better (stronger) rock mass conditions [Bieniawski, 1989; Bieniawski, 1993]. The first five factors are evaluated as a group and their values are

summed to give an unadjusted RMR value (from 0–100). The sixth parameter may be included separately as an adjustment to the RMR value [see Bieniawski, 1989, section B Table 4.1] because the influence of the orientation of the discontinuities has differing effects for various engineering applications, such as slope stability [Bieniawski, 1989]. In the study area, the joints do not show a strongly preferred orientation based on inspection of the azimuth-frequency relationship of these joints (Figure 2), so an additional adjustment for joint orientation is not included in the calculation of RMR.

[8] To determine UCS, a Microscopic Imager (MI) mosaic of a sample brushed by the rock abrasion tool (RAT) was used to measure grain size and porosity (Figure 3). The grain size of the intact rock material was determined to be below the resolution of the MI (31 $\mu\text{m}/\text{px}$), as individual grains inside the brushed area were not discernible. However, according to Grotzinger *et al.* [2005] and Squyres and Knoll [2005], the primary grain size of the particles from other areas ranges from 0.3 mm to 0.8 mm, which is defined as medium grained sand. The finer grained texture expressed at this site compared to others may be a result of the lesser degree of recrystallization from the multiple episodes of ground water influx [McLennan *et al.*, 2005; Squyres and Knoll, 2005]. As a result, we choose 31 μm as an upper limit to grain size at this site.

[9] Porosity is an important physical characteristic that strongly influences the strength and deformability of sedimentary rocks [Wong *et al.*, 2004]. A higher porosity reduces UCS and Young's modulus for sedimentary rocks [Chang *et al.*, 2006]. The porosity measurement reported here is restricted to the area without accumulations of surface dust, which were removed by the RAT brushing (Figure 3, area interior to the black circle).

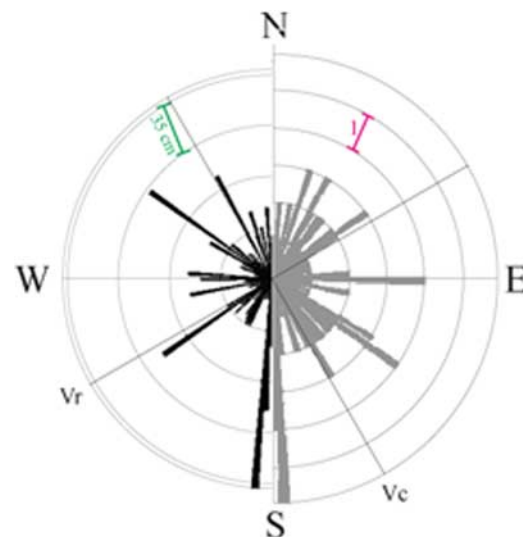


Figure 2. Joint orientations measured at study area (site 50) at Meridiani Planum. Right side (grey) shows azimuth-frequency relationship. Scale bar represents 1 joint. Left (black) shows summed length-azimuth relationship. Scale bar is 35 cm. Bin size is 2° for both halves. Number of joints, 101; Vr, azimuth of orientations radial to Vostok Crater (330°); Vc, azimuth of orientations concentric to Vostok Crater (60°).

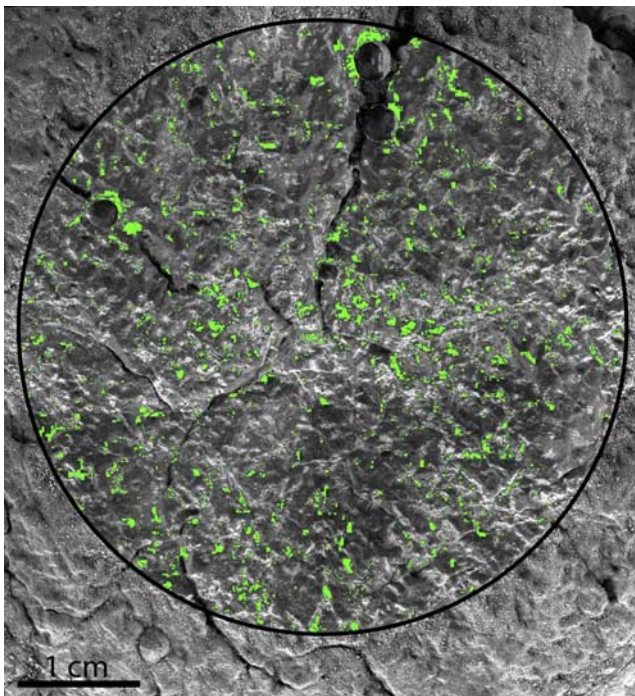


Figure 3. Microscopic Imager (MI) mosaic of RAT brushed target Gagarin. Green areas indicate location, size, and distribution of pores. Black circle represents brushed area and has a diameter of ~ 3.5 cm. Image courtesy of NASA/JPL/Cornell/USGS (<http://marsrovers.jpl.nasa.gov/gallery/press/opportunity/20050317a.html>).

[10] We assess the pre-alteration porosity of Burns Formation rock, here called primary porosity. The primary porosity of the intact rock material was determined through digital mapping of pore spaces [Okubo and Schultz, 2007] on the RAT brush MI target rock Gagarin. Pore spaces were identified by digitally selecting pixels with values that correspond with shadows and sunlit surfaces within the pores. This estimate was refined by manually adding pixels that fall within pores that were unselected previously and deleting pixels which are not primary pore space, such as fractures, vugs, and hematite concretions. Primary porosity is calculated as the ratio of the sum of selected pixels to the total number of pixels in the area contained within the black circle. The primary porosity at this location was determined to be 4.5%, representing the porosity during both past wet conditions as well as present-day dry conditions. Porosity measured in this way may be a lower bound because any pores below the resolution of the MI are not considered; on the other hand, dust removed by RAT brushing may have filled in some pores.

[11] A mechanical analog must be established before porosity measurements can be converted into values for strength and deformability. The amount of grind energy required by the RAT to grind targets is a measure of the mechanical strength of the rock. The amount of energy required to grind specific targets is given by Arvidson *et al.* [2004]. The grind energies for the outcrop we investigate here are consistent with, or less than, that obtained independently of dry terrestrial shale. While the mechanical response of the Burns Formation is similar to shale, the

materials that make up the Burns Formation are mineralogically different, with the sand-sized particles having formed from an evaporitic source [Grotzinger *et al.*, 2005]. The behavior of shale is therefore adopted as the appropriate mechanical analog for conversion of porosity measurements into estimates of strength and deformability.

[12] Without in situ measurements of Burns Formation, the unconfined compressive strength must be determined indirectly. The unconfined compressive strength (UCS) of the intact rock material was determined through the use of empirical equations for shale, which relate porosity to UCS [Chang *et al.*, 2006]. Using the primary porosity $\phi = 4.5\%$, equations 19 and 20 from Chang *et al.* [2006] give a range of UCS from 35–58 MPa. Given the variable fit of these equations to the original data [Chang *et al.*, 2006, Figure 2c], 50 MPa is used for the UCS in this study, giving a value of 5 points for this category of RMR. The full range of UCS associated with the calculated values gives a point range of 4–6 for this category, which corresponds to an insignificant $\pm 1\%$ change in the RMR values.

[13] Linear fracture spacing (eRQD) is the number of fractures per meter along a straight traverse line [Brady and Brown, 1993]. When performing an RMR analysis, the eRQD traverses are oriented perpendicular to the dominant joint set in order to maximize the number of joints intersecting the traverse line. Joints in the study area do not have a strongly preferred direction, but what appear to be systematic joints are oriented approximately north-south (Figure 2); the traverses were thus oriented east-west (Figure 1, inset). Outcrop properties should not be direction dependent due to the weak development of a preferred joint orientation. There may be a suggestion of a contribution from Vostok crater in the radial direction but a significant control of joint orientations by the crater is not apparent (Figure 2). eRQD for this outcrop is 8 joints per meter, for a value of 17 points of 20 for this category. Fracture spacing is calculated by dividing the length of the eRQD traverse by the number of joints that intersect it. Fracture spacing for this outcrop is 0.129 m, giving a value of 8 points out of the maximum 20 for this category.

[14] Joint condition is determined from joint aperture, filling, and morphology [Bieniawski, 1989, Table 4.1 or Chart E]. Joint length ranges from ~ 3 cm to ~ 1 m. Aperture is between 0.1–1 mm and the joints are filled with soft regolith (as also noted in other locations beyond the study area by Squyres *et al.* [2006]). The edges of the joints appear to be slightly rough, and have undergone moderate weathering. Summing the point values for these sub-parameters for joint condition gives a value of 18 of the maximum 30 for this parameter.

[15] Groundwater conditions affect the mechanical properties of the rock mass. Pore water pressure reduces rock mass strength and deformability. The outcrop is observed to be dry at present, but previous studies [e.g., Christensen *et al.*, 2004; Squyres *et al.*, 2004b; Grotzinger *et al.*, 2005; Squyres and Knoll, 2005] indicate that the unit was formed and altered in a wetter environment. Based on these studies, the past wet conditions were classified as ‘dripping’ from Bieniawski [1989, Table 4.1], for a value of 4 points of 15. In this context, the term ‘dripping’ refers to water under Artesian conditions and saturated with more movement than a stagnant pool of water at the surface, but with less velocity

Table 1. Physical Parameters for Burns Formation Rocks

Parameter	Description	Equation	Value
ϕ	Primary porosity		4.5%
R	Grain size		31 μm
RMR	Rock mass rating		63 (dry) 52 (wet)
m_i	Hoek-Brown parameter for intact rock material ^a		6 \pm 2
m	Hoek-Brown parameter for rock mass ^b	$m = m_i e^{\left(\frac{\text{RMR}-100}{14}\right)}$	0.427 (dry) 0.195 (wet)
s	Hoek-Brown parameter for rock mass ^c	$s = e^{\left(\frac{\text{RMR}-100}{6}\right)}$	0.0021 (dry) 0.00034 (wet)
E^*	In situ modulus of deformation for rock mass ^d	$E^* = 10^{\left(\frac{\text{RMR}-10}{40}\right)}$	21.1 GPa (dry) 11.2 GPa (wet)
C_0^*	Cohesive strength of rock mass ^e	$C_0 = \left(\frac{\sqrt{m^2+16s}-m}{4}\right) \left[\sigma_c^2 + \frac{16m\sigma_c}{(4\sqrt{s}-m+\sqrt{m^2+16s})^2}\right]^{\frac{1}{2}}$	4.64 MPa (dry) 3.12 MPa (wet)
T_0^*	Tensile strength of rock mass ^f	$T_0 = \frac{\sigma_c}{2} (m - \sqrt{m^2 + 4s})$	-0.24 MPa (dry) -0.09 MPa (wet)
P^*	Grain crushing pressure for intact rock material ^g	$P^* = \Gamma (\phi R)^{-0.5}$	19.5 GPa

^aValue for shale from *Marinos and Hoek* [2001].

^bEquation 7 from *Bieniawski* [1993].

^cEquation 8 from *Bieniawski* [1993].

^dEquation 3 from *Bieniawski* [1993].

^eEquation 10 after *Schultz* [1995].

^fEquation 4 from *Hoek and Brown* [1980].

^gEquation 2.9 from *Wong et al.* [2004].

than an aquifer under high pressures. For present-day dry conditions, the full value of 15 was assigned for this category. RMR for the outcrop is calculated as $5 + 17 + 8 + 18 + 4 = 52$ (wet case) and $5 + 17 + 8 + 18 + 15 = 63$ (dry case).

[16] In a porous rock or soil, critical pressure at the onset of grain crushing is defined as [*Wong et al.*, 2004, p. 85]

$$P^* = \Gamma(\phi R)^{-0.5} \quad (1)$$

where Γ is a coefficient approximately equal to 1 [*Wong et al.*, 2004], ϕ is the porosity expressed as a decimal, and R is the grain radius in mm. Mineralogical analyses [*Clark et al.*, 2005] show that the material of the Burns Formation is analogous to a chemically altered Martian basalt. However, P^* for analogous terrestrial evaporate material has not been measured in the laboratory. Using values of grain size ($R = 31 \mu\text{m}$) and primary porosity ($\phi = 0.045$) for the Burns Formation exposure in (1), P^* is calculated to be 19.5 GPa. Because (1) assumes hard quartz grains in contact, the critical pressure calculated here may be overestimated by perhaps an order of magnitude.

[17] Rock mass strengths, including tensile and cohesive, are calculated by using the parameters m_i , m , and s along with the values of RMR. Following *Hoek* [1983], m characterizes the slope of the Mohr envelope and s is the squared ratio of the unconfined compressive strength of the rock mass to the UCS of the intact rock material [*Hoek and Brown*, 1980, equation 3]. We adopt values for m_i of 6 ± 2 , appropriate for terrestrial shales and evaporites [*Marinos and Hoek*, 2001] (Table 1). The largest uncertainty in the calculated strength values, related to that in the values of m for the intact rock material (m_i), is $\sim\pm 30\%$; as a result, the calculated strength values are considered accurate within a factor of 2. Uncertainty in the RMR values is $\sim 10\%$, with uncertainty coming from the estimate of the groundwater

conditions ('dripping,' wet case only) and to a lesser extent joint conditions (both wet and dry cases).

4. Discussion and Conclusions

[18] RMR values were calculated for both environments. The RMR for past wet conditions was determined to be 52, while RMR was 63 for present day dry conditions. Accounting for water reduces all values dependent on RMR (Table 1). The upper unit of the Burns Formation thus has properties of RMR, strength, and deformability that are comparable to those of terrestrial sedimentary rock masses such as siltstone, sandstone, mudstone, and shale [e.g., *Bieniawski*, 1989; *Somnez et al.*, 1998].

[19] Application of this method to other outcrops of the Burns Formation would allow for determination of the degree of spatial variation of physical properties, such as porosity, unconfined compressive strength, and degree of jointing, of a geologic unit on Mars. In addition, application to outcrops imaged by *Opportunity's* sister rover, *Spirit*, at Gusev crater would allow for analysis of other rock types for Mars, such as basaltic lava flows, motivating a global generalization of rock properties of Martian basaltic and sedimentary rocks.

[20] Understanding the physical properties of Martian materials on the outcrop scale would allow for a greater understanding of the range of types and distribution of materials present on Mars' surface. It may also facilitate understanding of the changes in geological processes, both on Mars' surface and in the Martian interior, through time.

[21] **Acknowledgments.** We thank the two anonymous reviewers for their helpful comments that sharpened the final paper, Shane Thompson and Wendy Calvin for assistance and advice with the MER data, and Marjorie Chan for discussions about desiccation cracks. This work was supported by a grant from NASA's Mars Data Analysis Program to RAS.

References

- Arvidson, R. E., et al. (2004), Localization and physical property experiments conducted by Opportunity at Meridiani Planum, *Science*, *306*, 1730–1733.
- Bieniawski, Z. T. (1989), *Engineering Rock Mass Classifications*, Wiley, Chichester, U. K.
- Bieniawski, Z. T. (1993), Classification of rock masses for engineering: The RMR system and future trends, in *Comprehensive Rock Engineering: Principles, Practice, and Projects*, vol. 3, edited by J. A. Hudson, pp. 553–573, Pergamon, Oxford, U. K.
- Brady, B. H. G., and E. T. Brown (1993), *Rock Mechanics for Underground Mining*, 2nd ed., 571 pp., Chapman and Hall, London.
- Chan, M. A., et al. (2007), Polygonal cracking and “Wopmay” weathering patterns on Earth and Mars: Implications for host-rock properties, paper presented at 38th Annual Lunar and Planetary Science Conference, Lunar Planet. Inst., Houston, Tex., 12–16 Mar.
- Chang, C., et al. (2006), Empirical relations between rock strength and physical properties in sedimentary rocks, *J. Petrol. Sci. Eng.*, *51*, 223–237.
- Christensen, P. R., et al. (2004), Mineralogy at Meridiani Planum from the Mini-TES Experiment on the Opportunity Rover, *Science*, *306*, 1733–1739.
- Clark, B. C., et al. (2005), Chemistry and mineralogy of outcrops at Meridiani Planum, *Earth Planet. Sci. Lett.*, *240*, 73–94.
- Grotzinger, J. P., et al. (2005), Stratigraphy and sedimentology of a dry to wet eolian depositional system, Burns Formation, Meridiani Planum, Mars, *Earth Planet. Sci. Lett.*, *240*, 11–72.
- Grotzinger, J. P., et al. (2006), Sedimentary textures formed by aqueous processes, Erebus crater, Meridiani Planum, Mars, *Geology*, *34*(12), 1085–1088, doi:10.1130/G22985A.1.
- Hoek, E. (1983), Strength of jointed rock masses, 23rd Rankine Lecture, *Géotechnique*, *33*(3), 187–223.
- Hoek, E., and E. T. Brown (1980), Empirical strength criterion for rock masses, *J. Geotech. Eng. Div. Am. Soc. Civ. Eng.*, *106*(GT9), 1013–1035.
- Hynek, B. M., R. E. Arvidson, and R. J. Phillips (2002), Geologic setting and origin of Terra Meridiani hematite deposit on Mars, *J. Geophys. Res.*, *107*(E10), 5088, doi:10.1029/2002JE001891.
- Marinos, P., and E. Hoek (2001), Estimating the geotechnical properties of heterogeneous rock masses such as flysch, *Bull. Eng. Geol. Environ.*, *60*, 85–92.
- McLennan, S. M., et al. (2005), Provenance and diagenesis of the evaporite-bearing Burns Formation, Meridiani Planum, Mars, *Earth Planet. Sci. Lett.*, *240*, 95–121.
- Neuffer, D. P., and R. A. Schultz (2006), Mechanisms of slope failure in Valles Marineris, Mars, *Q. J. Eng. Geol. Hydrogeol.*, *39*, 227–240.
- Okubo, C. H., and R. A. Schultz (2004), Mechanical stratigraphy in the western equatorial region of Mars based on thrust fault-related fold topography and implications for near-surface volatile reservoirs, *Geol. Soc. Am. Bull.*, *116*, 594–605.
- Okubo, C. H., and R. A. Schultz (2007), Compactional deformation bands in Wingate Sandstone: Additional evidence of an impact origin for Upheaval Dome, Utah, *Earth Planet. Sci. Lett.*, *256*, 169–181.
- Pollard, D. D., and A. Aydin (1988), Progress in understanding jointing over the last century, *Geol. Soc. Am. Bull.*, *100*, 1181–1204.
- Schultz, R. A. (1995), Limits on strength and deformation properties of jointed basaltic rock masses, *Rock Mech. Rock Eng.*, *28*(1), 1–15.
- Somnez, H., et al. (1998), A practical procedure for the back analysis of slope failures in closely jointed rock masses, *Int. J. Rock Mech. Min. Sci.*, *35*, 219–233.
- Squyres, S. W., and A. H. Knoll (2005), Sedimentary rocks at Meridiani Planum: Origin, diagenesis, and implications for life on Mars, *Earth Planet. Sci. Lett.*, *240*, 1–10.
- Squyres, S. W., et al. (2004a), The Opportunity Rover’s Athena science investigation at Meridiani Planum, Mars, *Science*, *306*, 1698–1703.
- Squyres, S. W., et al. (2004b), In situ evidence for an ancient aqueous environment at Meridiani Planum, Mars, *Science*, *306*, 1709–1714.
- Squyres, S. W., et al. (2006), Two years at Meridiani Planum: Results from the Opportunity Rover, *Science*, *313*, 1403–1407.
- Wong, T.-F., et al. (2004), Mechanical compaction, in *Mechanics of Fluid-Saturated Rocks*, edited by Y. Guéguen and M. Boutéca, pp. 55–114, Elsevier Acad., Amsterdam.

A. L. Nahm and R. A. Schultz, Geomechanics-Rock Fracture Group, Department of Geological Sciences and Engineering, University of Nevada, Reno, MS 172, Reno, NV 89557, USA. (nahma@mines.unr.edu)